THE ASTROPHYSICAL JOURNAL, 354:L57–L60, 1990 May 10

THE Ni/Fe RATIO IN THE CRAB NEBULA

DOUGLAS HUDGINS[1] AND TERRY HERTER[1]
Cornell University
AND
RICHARD J. JOYCE
Kitt Peak National Observatory,[2] National Optical Astronomy Observatories
Received 1990 January 25; accepted 1990 February 27

ABSTRACT

We present spectrophotometric observations of the [Ni II] 1.191 μm and [Fe II] 1.257 μm lines at position 10 of Fesen and Kirshner in the Crab Nebula. To our knowledge, this is the first detection of the 1.19 μm line in a Galactic supernova remnant. Both lines are located in spectral regions relatively free of atmospheric absorption and airglow emission, and no confusion with other astrophysical lines exists. This makes these lines excellent probes of warm, low-excitation interstellar environments.

Adopting an electron temperature of 16,000 K and an electron density of 850 cm^{-3}, based on optical studies of the gas, we derive an Ni/Fe ratio of 0.3. This ratio is about a factor of 6 higher than the solar ratio but is significantly smaller than the Ni/Fe ratio derived from the [Ni II] 0.7378 and [Fe II] 0.8617 μm lines which yield Ni/Fe ratios of 50–75 times solar. Both of these ratios can be reconciled by increasing the electron density by a factor of $\sim$10. The derived Ni/Fe ratio from optical lines is left unchanged, while the ratio computed from infrared lines is increased by more than a factor of 4. However, such high densities seem physically implausible given the constraints placed on the conditions in the filaments from other observed lines. It is more likely that the atomic data for either Ni or Fe or both are in error causing the infrared and optical abundance ratios to disagree.

Subject headings: nebulae: abundances — nebulae: Crab Nebula — nebulae: supernova remnants — spectrophotometry

I. INTRODUCTION

Recent observations have indicated an anomalously high nickel-to-iron ratio in the filaments of the Crab Nebula (see Dennefeld and Péquignot 1983; Henry 1984; MacAlpine *et al.* 1989). These results, based on measurements of the [Ni II] 0.7378 μm and [Fe II] 0.8617 μm lines, suggest that the Ni/Fe ratio is a factor of 50–75 greater than the solar ratio. Moreover, in an analysis of data on other supernova remnants, Dennefeld (1986) again finds high Ni/Fe ratios, although the Crab Nebula seems to be the most extreme example. Henry (1984) also finds the Ni/Fe ratio is 17 times solar in the Orion Nebula. Understanding the origin of this high ratio is important for making reliable estimates of the heavy element abundances in supernova remnants and other environments.

Several explanations can account for the large derived Ni/Fe ratio. Suggestions have included (1) preferential depletion of Fe into grains, (2) errors in the atomic data for Ni or Fe, (3) the presence of material processed under neutron-rich conditions, (4) large charge exchange or dielectronic recombination rates affecting the ionic fractions or populations of the levels of Ni^+ or Fe^+, or (5) preferential excitation of the [Ni II] 0.7378 μm line through a fluorescence (or other) mechanism. Henry (1984) has discussed this problem in detail and favors a large charge exchange or dielectronic recombination rate for the production of Ni^+. He has also suggested that Ni lines in the infrared can test whether electron-ion collisions are responsible for exciting the optical transitions (Henry 1987). Observing other lines can also serve as a check on the accuracy of the atomic data for Ni and Fe. Henry and Fesen (1988) have argued that the presence of a strong [Ni II] 0.7378 μm line in many different types of objects argues against a large nickel abundance.

Assuming collisional excitation by electrons, Henry (1987) solved for the populations of the 17 level Ni^+ ion over a range of temperatures and densities. Using present information on the physical conditions of the emission region and the observed strength of the [Ni II] 0.7378 μm line, he finds that several Ni II lines in the infrared should be comparable in brightness to the 0.7378 μm line. These lines are located at 1.19, 6.63, and 10.7 μm. Unfortunately, observing sensitivity at 6.63 and 10.7 μm is severely limited by the high thermal background from the atmosphere. In addition, the 6.63 μm line can be detected only from airborne or space-based platforms. The low background conditions present at 1.19 μm make observations of this line much more tenable.

Thus, we undertook a program to measure the [Ni II] 1.19 μm line in the Crab Nebula to investigate whether the 0.7378 μm transition is artificially enhanced or, possibly, the atomic data for Ni (or Fe) are in error. We detected both the [Ni II] 1.19 μm and [Fe II] 1.26 μm lines, permitting a direct determination of the Ni/Fe ratio from infrared data alone, and providing an independent comparison with the optical data.

II. OBSERVATIONS

The Crab Nebula was observed during two nights in 1988 November using the infrared grating array spectrometer (CRSP) mounted on the KPNO 1.3 m telescope. This instru-

[1] Visiting Astronomer, Kitt Peak National Observatory, operated by the Association of Universities for Research in Astronomy, Inc., under cooperative agreement with the National Science Foundation.

[2] Operated by the Association of Universities for Research in Astronomy, Inc., under cooperative agreement with the National Science Foundation.

ment employs a 62 × 58 InSb array to provide spectral information in one direction and spatial sampling in the other direction. The spatial scale is 2.″7 per pixel giving an unvignetted slit size of about 2′ in the cross-dispersion direction. The spectral resolution is determined by the slit width for an extended source. The dispersion is about 0.001 μm per pixel yielding a spectral resolution of ~0.0025 μm for the 7″ slit width that was used.

Spectrophotometric observations were performed with the slit oriented north-south and centered at position 10 of Fesen and Kirshner (1982), hereafter FK10. This position is located 60″ south and 30″ east of star 16 of Wyckoff and Murray (1977). It was expected to be one of the brighter filaments in the nickel line based on optical observations (see Henry 1987). The setting of the slit position by this procedure should be accurate to better than an arcsecond. Spectra were obtained at 1.19 μm, the expected position of the [Ni II] line, and at 1.27 μm which allowed both the Paβ 1.28 μm and [Fe II] 1.26 μm lines to be measured simultaneously.

For each integration on-source, a background exposure of equal duration was also taken 180″ east of the filament. Exposure times of 1200 and 500 s were used at 1.19 μm and 1.27 μm, respectively. The background spectra were subtracted from the corresponding on-source exposures to remove bias offsets, dark current, and sky emission. Bad pixels were removed through redundant sampling. After the spectrum was measured at the nominal line position, the grating was moved to shift the spectrum by 5 pixels on the array. Another series of on-source and background exposures was then performed. Spectra at different grating positions were combined to remove bad pixels. One-dimensional spectra were extracted over a region 30″ in the cross-dispersion direction.

BS 1552 (B2 III) served as the primary calibrator. The region near Paβ was ignored since the star has an intrinsic absorption line at this position. According to the KPNO photometric calibration, a J-band magnitude of 4.04 was adopted. Using the CIT zero magnitude flux calibration, we adopt fluxes of 8.6×10^{-8} and 6.8×10^{-8} ergs cm^{-2} s^{-1} μm^{-1} for BS 1552 at 1.19 and 1.28 μm, respectively.

Figures 1 and 2 show the calibrated spectrophotometric data for the Ni II and Paβ line positions. A line at 1.191 μm which we associate with [Ni II] is quite evident in Figure 1. A strong [Fe II] 1.257 μm line and the Paβ 1.282 μm line are also detected (Fig. 2). A weak emission line at 1.294 ± 0.001 μm also appears to be present. As we discuss later, this line could be due to Fe II. Both the Paβ and the 1.294 μm lines lie very near atmospheric emission features, and hence the line fluxes are very dependent on the accuracy of the background subtraction procedure. The lower panels of Figures 1 and 2 show the atmospheric emission in the bands observed. These spectra were produced by subtracting dark frames from the off-source sky positions, flat-fielding, and combining spectra. Most of the emission is due to OH (see Steed and Baker 1979), and these lines were used as the primary wavelength calibration.

Both the [Ni II] 1.19 μm and [Fe II] 1.26 μm transitions occur in relatively clear parts of the spectrum. Neither is significantly contaminated by strong atmospheric emission lines (see Figs. 1 and 2). By contrast, the proximity of atmospheric line emission to the Paβ and 1.294 μm lines is evident. Although the airglow lines appear to subtract out very well, it should be remembered that contamination of these two weak lines may exist.

Gaussian fits to the lines are shown in Figures 1 and 2, and

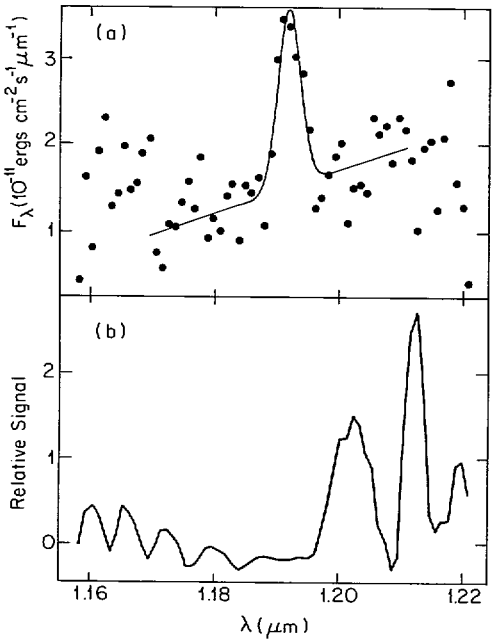

FIG. 1.—(*a*) Spectrum of Crab Nebula obtained at position FK10 (Fesen and Kirshner 1982) showing the [Ni II] 1.191 μm line. The solid line indicates a Gaussian fit to the line. The spectral resolution is approximately 0.001 μm, and the extracted slit size is 7″ × 30″ with the orientation north-south. (*b*) Night sky emission spectrum measured 180″ east of FK10. The OH emission lines served as a wavelength calibration.

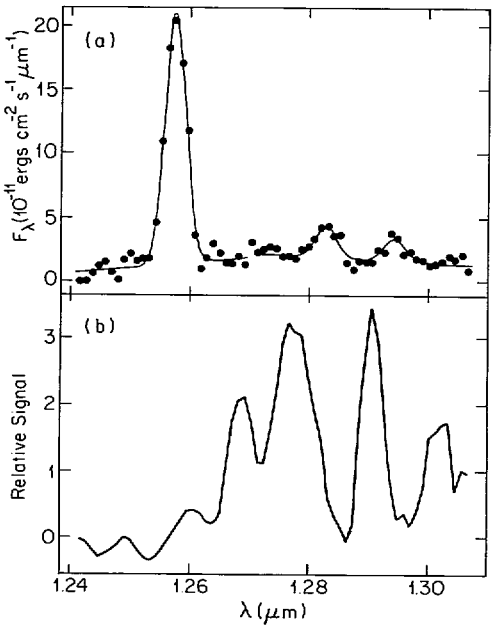

FIG. 2.—(*a*) Spectrum of Crab Nebula obtained at position FK10 (Fesen and Kirshner 1982) showing [Fe II] 1.257 and 1.294 μm, and Paβ 1.282 μm lines. Gaussian fits to the line profiles are shown as solid lines. The spectral resolution is approximately 0.001 μm, and the extracted slit size is 7″ × 30″ with the orientation north-south. (*b*) Night sky emission spectrum measured 180″ east of FK10. Both OH and O_2 emission lines are present. The OH lines were used as a wavelength calibration.

TABLE 1

CRAB FILAMENT LINE FLUXES[a]

LINE	λ[b] (μm)	$\Delta\lambda$ (μm)	FLUX (10^{-14} ergs cm^{-2} s^{-1}) Measured	Corrected
Ni II	1.192 ± 0.001	0.0042 ± 0.0005	9.3 ± 1.6	14.2 ± 2.4
Paβ	1.283 ± 0.001	0.0041 ± 0.0007	10.9 ± 2.4	15.9 ± 3.5
Fe II	1.258 ± 0.001	0.0040 ± 0.0002	83.0 ± 4.0	124.0 ± 6.0
	1.294 ± 0.001	0.0041	7.6 ± 1.3	10.9 ± 1.9

[a] Data obtained at position 10 of Fesen and Kirshner 1982 with a 7″ × 2′ slit oriented north-south. The lines fluxes are derived from data in the central 30″ of the slit.

[b] Fitted line position using wavelength calibration based on atmospheric OH emission. The actual wavelength of Paβ is 1.2818 μm.

fluxes are given in Table 1. Using $E(B-V) = 0.5$ to the Crab Nebula (Miller 1978; Wu 1981) and adopting the extinction curve of Rieke and Lebofsky (1985; see also Draine 1989), corrected line fluxes are also given in Table 1. The quoted flux errors are statistical errors and hence do not reflect systematic calibration errors. The overall calibration is probably accurate to 15%–25%.

III. RESULTS

a) *Line Comparisons*

Graham, Wright, and Longmore (1990) have measured the [Fe II] $a\,^4D_{7/2}$–$a\,^4F_{9/2}$ 1.644 μm line. Since this line originates from the same upper level as the [Fe II] $a\,^4D_{7/2}$–$a\,^6D_{9/2}$ 1.257 μm transition, the expected flux ratio is just determined by the branching ratio for the two transitions. From the data of Nussbaumer and Storey (1988), we expect the emissivity ratio to be $j(1.26)/j(1.64) = 1.27$. Using the dereddened 1.64 μm line flux from Graham, Wright, and Longmore, we expect a flux of $108 \pm 3 \times 10^{-14}$ ergs cm^{-2} s^{-1} for the 1.26 μm line. This is about 15% lower than our measured flux (Table 1) but well within the expected calibration errors.

There is an indication of a weak line located near Paβ at 1.294 μm. Although our fit indicates this line is statistically significant ($>5\,\sigma$), it should be kept in mind that the line falls very close to a bright OH atmospheric emission feature (see Fig. 2). In general, the removal of the atmospheric emission appears quite good, but an additional complication is that one of the background positions is in a bad region of the array. Thus, we will proceed with an identification and analysis using the 1.294 μm line but caution should be exercised in overinterpreting the results.

A natural candidate for the 1.294 μm line is Fe II since it has many lines occurring in the near-infrared. In addition to the 1.26 μm line, Fe II transitions occur near Paβ at 1.271, 1.279, and 1.294 μm (Nussbaumer and Storey 1988). In order to determine the strengths of these lines relative to the 1.26 μm line we solved for the level populations of the 16 lowest levels of the Fe II ion assuming collisional excitation by electrons. Emissivities were then calculated over a range of electron temperatures and densities using the atomic data of Nussbaumer and Storey (1980, 1988). Figure 3 shows the strengths of these three lines relative to the 1.26 μm line. The 1.294 μm is the brightest of the three and varies from 0.02 to 0.3 times the intensity of the 1.26 μm line depending on the density. From the observed line ratio, we estimate an electron density of ~ 5000 cm^{-3}; however, this estimate is not very accurate (see Fig. 3).

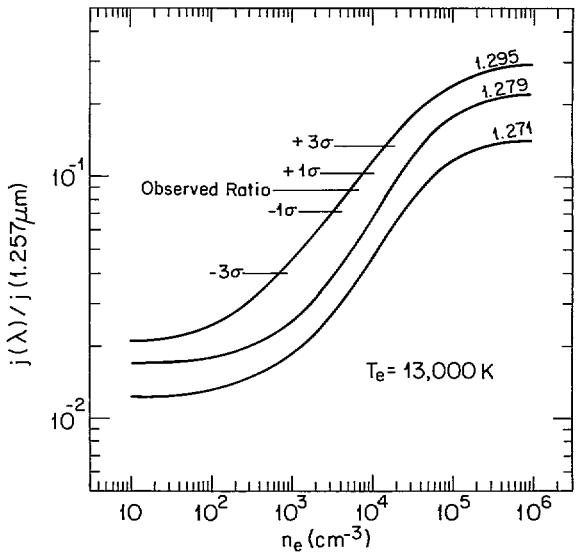

FIG. 3.—Emissivity of the [Fe II] 1.294, 1.279, and 1.271 μm lines relative to the [Fe II] 1.257 μm lines as a function of electron density computed from the data of Nussbaumer and Storey (1980, 1988). The assumed electron temperature is 13,000 K; however, the ratios change by less than 10% for temperatures between 5000 and 18,000 K. The observed [Fe II] 1.294/1.257 line ratio and error bars are also shown.

b) *The* Ni/Fe *Ratio*

Detailed models (see Henry and MacAlpine 1982; Péquignot and Dennefeld 1983) of the filaments in the Crab Nebula indicate that emission from high-ionization species such as O III arise from the H^+ zone, whereas the [O II] and [S III] line emission come from near and within the $H^+ \rightarrow H^0$ transition zone. [S II], [Fe II], and [Ni II] emission emanate from the H^0 region (for further discussion see Henry, MacAlpine, and Kirshner 1984). The discovery of copious H_2 emission from filaments also indicates the presence of significant amounts of molecular gas (Graham, Wright, and Longmore 1990).

Differences in the relative strengths of emission lines between filaments can arise from variations in the ionizing flux or local abundance changes. Uomoto and MacAlpine (1987) find regions of high and low helium emission relative to hydrogen. From long-slit spectroscopy MacAlpine *et al.* (1989) confirm that in some locations the gas is ~95% helium by mass. The filament, FK10, which we measure here does not appear to have such a high helium fraction. Although the He/H ratio appears to vary considerably throughout the nebula, the Ni/Fe ratio as measured by the [Ni II] 0.7378 μm and [Fe II] 0.8617 μm lines is relatively constant. Typical derived Ni/Fe ratios are 50–75 times the solar ratio (MacAlpine *et al.* 1989; Henry 1987).

In order to compute a Ni/Fe ratio from our measurements, we must have a density estimate for the emission region. Fesen and Kirshner (1982) estimate an electron density of 850 ± 400 from [S II] line ratios. As discussed above, since the Ni II, Fe II, and S II zones are expected to coincide, this density should be applicable to the [Ni II] and [Fe II] emission lines. The electron temperature, T_e, as determined from [O III] and [O II] lines is 16,000 ± 3000 K (Miller 1978; Fesen and Kirshner 1982). Neither of these lines is thought to originate from the same region as Ni II and Fe II lines. S II measurements give $T_e = 7500 \pm 1500$ K, but these lines may be blended with [Fe III] or [Fe V] lines and hence provide an unreliable tem-

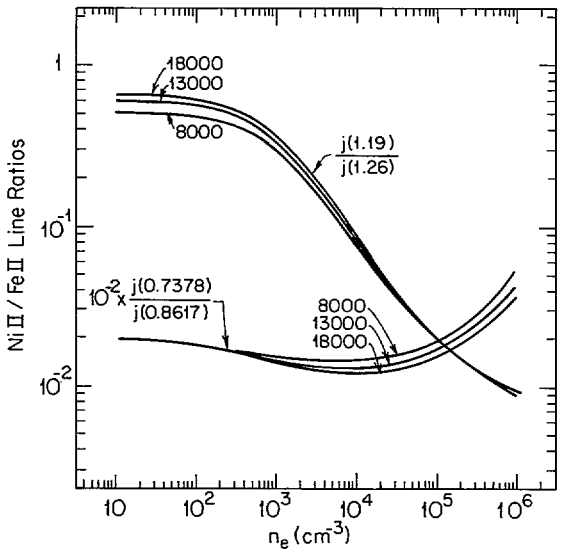

FIG. 4.—Emissivity ratios per ion of [Ni II] 1.191 μm/[Fe II] 1.257 μm and [Ni II] 0.7378 μm/[Fe II] 0.8617 μm lines vs. electron density for various electron temperatures. The 0.7378/0.8617 line ratio has been multiplied by a factor of 0.01. The atomic data of Nussbaumer and Storey (1980, 1982, 1988) have been used.

perature estimate (see Fesen and Kirshner 1982). Figure 4 shows the ratio of the [Ni II] 1.19 μm to [Fe II] 1.26 μm emissivity per ion as a function of density for different temperatures. The temperature dependence of the ratio is very weak. For a variation in T_e from 16,000 K to 8000 K, the range of temperatures discussed above, the 1.19/1.26 μm line emissivity ratio changes by only 15%. We will adopt T_e = 16,000 K, recognizing that this value may be high, but the choice of T_e has little impact on our estimated abundance ratio.

Using our measured [Ni II] 1.19 μm and [Fe II] 1.26 μm dereddened line fluxes we derive a Ni/Fe ratio of 0.30 $\pm$ 0.08 by number. This ratio is about a factor of 6 higher than the solar value (Ni/H = 1.8×10^{-6} and Fe/H = 3.4×10^{-5} by number; Cameron 1982). However, our value of Ni/Fe is much less than the factor of 50–75 deduced from measurements of the [Ni II] 0.7378 μm and [Fe II] 0.8617 μm (Dennefeld and Péquignot 1983; Henry 1984; MacAlpine *et al.* 1989).

IV. DISCUSSION

What is the cause of the discrepancy between the infrared and optical determinations of the Ni/Fe ratio? Figure 4 displays ratios of the emissivity per ion for both the [Ni II] 1.19/[Fe II] 1.26 μm and [Ni II] 0.7378/[Fe II] 0.8617 μm lines as a function of electron density. Whereas the shorter wavelength line ratio is nearly independent of density, the emissivity ratio of the infrared lines decreases linearly with density for densities above 1000 cm^{-3}. If the density were increased from the adopted value of 850 cm^{-3} to 10,000 cm^{-3}, j(1.19)/j(1.26) decreases by about a factor of 5. This increases the deduced Ni/Fe ratio by the same factor.

The electron density we deduce by matching the optical and infrared Ni/Fe ratios is over a factor of 10 higher than that determined from S II studies of Fesen and Kirshner (1982). Is such a high electron density reasonable? An immediate requirement would be the separation of the S II zone from the Ni II and Fe II zones. The usual assumption is that these ionization zones overlap and fall within the H^0 region (see Henry 1984). Unless this assumption is incorrect, it is unlikely that anomalously high electron densities are the cause of the difference between the two determinations of the Ni/Fe ratio.

If there are problems with the atomic data for Ni II or Fe II, then either or both of the deduced Ni/Fe ratios could be in error. Typically, transition probabilities are much more accurately known than collision strengths. Nussbaumer and Storey (1988) have recently recalculated the transition probabilities for Fe II, changing some of the previous values by up to a factor of 2. Calculations of collision strengths for Fe II by Baluja, Hibbert, and Mohan (1986) differ by up to a factor of 2 from those of Nussbaumer and Storey (1980); however, Nussbaumer and Storey (1988) question the accuracy of the results of Baluja *et al.* because a resonance which occurs in their calculations may not be physically realistic. Based on the line comparisons above and in view of the recent recalculations of the Fe II atomic parameters, it seems most likely that the factor of 8–12 discrepancy between the optical and infrared determinations of the Ni/Fe ratio is due to a significant error in the Ni II atomic data (although a fluorescence-like mechanism to enhance the [Ni II] 0.7378 μm line cannot be ruled out by our measurements). Recalculation of both the transition probabilities and collision strengths for Ni II is needed to resolve the issue of the Ni/Fe abundance in Galactic supernova remnants and elsewhere.

REFERENCES

Baluja, K. L., Hibbert, A., and Mohan, M. 1986, *J. Phys. B*, **19**, 3613.
Cameron, A. G. W. 1982, in *Essays in Nuclear Astrophysics*, ed. C. A. Barnes, D. D. Clayton, and D. N. Schramm (Cambridge: Cambridge University Press), p. 23.
Dennefeld, M. 1986, *Astr. Ap.*, **157**, 267.
Dennefeld, M., and Péquignot, D. 1983, *Astr. Ap.*, **127**, 42.
Draine, B. T. 1989, in *Proc. of the 22nd ESLAB Symposium: Infrared Spectroscopy in Astronomy*, ed. M. Kessler (Noordwijk: ESA), in press.
Fesen, R. A., and Kirshner, R. P. 1982, *Ap. J.*, **258**, 1.
Graham, J. R., Wright, G. S., and Longmore, A. J. 1990, *Ap. J.*, **352**, 172.
Henry, R. B. C. 1984, *Ap. J.*, **281**, 644.
———. 1987, *Ap. J.*, **322**, 399.
Henry, R. B. C., and Fesen, R. A. 1988, *Ap. J.*, **329**, 693.
Henry, R. B. C., and MacAlpine, G. M. 1982, *Ap. J.*, **258**, 11.
Henry, R. B. C., MacAlpine, G. M., and Kirshner, R. P. 1984, *Ap. J.*, **278**, 619.
MacAlpine, G. M., McGaugh, S. S., Mazzarella, J. M., and Uomoto, A. 1989, *Ap. J.*, **342**, 364.
Miller, J. 1978, *Ap. J.*, **220**, 490.
Nussbaumer, H., and Storey, P. J. 1980, *Astr. Ap.*, **89**, 308.
———. 1982, *Astr. Ap.*, **110**, 295.
———. 1988, *Astr. Ap.*, **193**, 333.
Péquignot, D., and Dennefeld, M. 1983, *Astr. Ap.*, **120**, 249.
Rieke, G. H., and Lebofsky, M. J. 1985, *Ap. J.*, **288**, 618.
Steed, A. J., and Baker, D. J. 1979, *Appl. Optics*, **18**, 3386.
Uomoto, A., and MacAlpine, G. M. 1987, *A.J.*, **93**, 1511.
Wu, C.-C. 1981, *Ap. J.*, **245**, 581.
Wyckoff, S., and Murray, C. A. 1977, *M.N.R.A.S.*, **180**, 717.

T. HERTER: Center for Radiophysics and Space Research, Space Sciences Building, Ithaca, NY 14853

D. HUDGINS: Department of Chemistry, Space Sciences Building, Ithaca, NY 14853

R. J. JOYCE: Kitt Peak National Observatory, P.O. Box 26732, Tucson, AZ 85726